

Application of modified Maple Wood Saw Dust with Polyaniline for the Removal of Anionic Dyes From Waste water : Kinetics and Isotherm Studies

A.A. Emam*, Nora M Hilal, A. A. El-Bayaa, N.A. Badawy, and U.A. Ghiat
Chemistry Department, Faculty of Science, Al-Azhar University (Girls), Nasr City, Cairo, Egypt

* a_a_emam@yahoo.com

Abstract:

In this work, application of polyaniline coated onto wood sawdust (PAni/SD) for the removal of anionic dyes namely Reactive Red 43 (RR43 dye) and Direct Orange 85 (DO85 dye) from aqueous solutions is introduced. Maple wood sawdust was characterized by Fourier Transform-Infrared Spectroscopy (FTIR), Scanning Electron Microscopy (SEM). The effects of some important parameters such as pH, initial concentration, sorbent dosage, and contact time on the uptake of anionic dyes solution were also investigated. In order to get a better comparison, adsorption experiments were also carried out using polyaniline coated maple wood saw dust (PAni/MWSD) and without coating (MWSD). It was found that PAni/MWSD can be used to remove anionic dyes such as DO85 and RR43 dyes from aqueous solutions very efficiently. Experimental data were analyzed by the Langmuir, Freundlich and Temkin models of adsorption. Kinetic parameters for the adsorption of anionic dyes for the selected adsorbents are also reported. Application of modified sawdust with polyaniline for the removal of anionic dyes is very promising for wastewater treatment.

Keywords: MWSD, polyaniline coated MWSD, anionic dyes, adsorption, kinetics and isotherm studies.

1. Introduction

Totally, 280,000 tons of 10,000 different classes of annually consumed dyes in textile industry and dye houses are introduced into the environment by either direct discharging or during subsequent textile processes (Goeset *et al.*, 2016; Maas and Chaudhari, 2005). This is while, only small concentration of dyes, i.e. about 1 ppm, is high enough to affect water quality (Crini, 2006; Rafatullah *et al.*, 2010). Common wastewater purification systems have low efficiency in some classes of anionic dyes such as reactive and acidic dyes, while they are also resistant against aerobic degradation (Robinson *et al.*, 2001). In addition, other processes such as ozonation, reverse osmosis, coagulation and flocculation suffer from problems including cost limitations and sludge production. Further, some of the mentioned processes are not practical in low dye concentration levels (Lee *et al.*, 2016).

Nowadays, economic and environmental friendly approaches such as adsorbing to refine wastewater have found great attention. In this regard, nylon-polyaniline nanocomposite web with high dye desorption capacity is developed. This is implemented through in-situ polymerization of polyaniline on the surface of electrospun nylon-6 nanofibers (Kamran Zarrini, *et al.*, 2017). Polyaniline is one of the most studied conductive polymers with high environmental and thermal stability which have found many applications. This polymer can be easily synthesized through achemically/electrochemically oxidative polymerization process (Chen *et al.*, 2011a; Jaymand, 2013; Syed and Dinesan, 1991).

The by-products from the forestry and agricultural industries could be assumed to be low-cost adsorbents since they are abundant in nature, inexpensive, require little processing and are effective materials. Saw dust is an abundant by-product of the wood industry that is either used as cooking fuel or as packing material (Garget *et al.*, 2004). Saw dust is easily available at negligible price. The role of saw dust materials in the removal of pollutants from aqueous solutions has been reviewed recently (Shukla *et al.*, 2002). Sawdust has proven to be a promising effective material for the removal of various dyes. (Venkat and Vijay Babu, 2013).

Hence in the present study, the maple wood saw dust considered to be a waste has been used effectively as an adsorbent. Thus the prepared polyaniline coated sawdust was used as an adsorbent for the removal of two different types of dyes namely Reactive Red 43 and Direct Orange 85 from aqueous solutions. The study includes an evaluation of the effects of various parameters like initial dye concentration, contact time and pH. The adsorption kinetic models, equilibrium isotherm models related to adsorption process were a slope formed and reported.

2. Experimental

2.1. Adsorbents (Maple wood sawdust)

Maple wood sawdust samples were collected from a local Damietta Port - Egypt. The maple wood sawdust samples were sieved through 0.355 mm and it was used directly for adsorption experiments without any physical and chemical treatments.

The sawdust supplied by a local wood processing factory was washed with distilled water to remove impurity, and then dried overnight at 60°C. The dried sawdust was sieved to retain the 0.355 mm fractions for further chemical synthesis. 140 mL of HCl concentrated (Merck, Germany) was added to 10 g of sawdust.



2.2. Preparation of PANi/SD and adsorption experiments

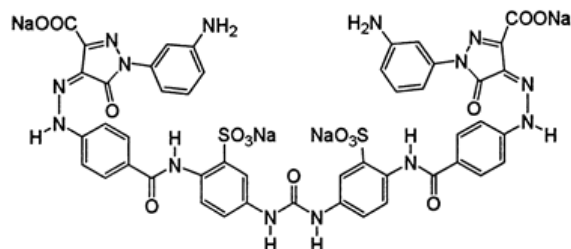
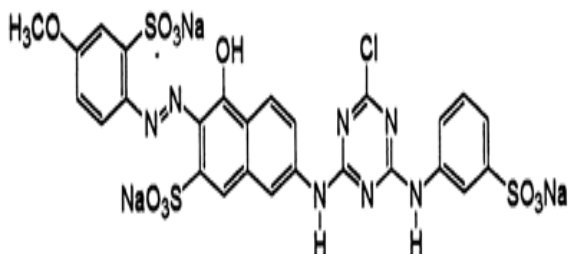
Sawdust (5.0 g, 0.355mm, 10 % humidity) was immersed in an aqueous aniline solution (0.2 M, 100 mL) for 12 h before polymerization. The excess of the monomer solution was removed by simple decantation. The amount of 50 mL of the oxidant solution, an aqueous solution (0.2 M) of $(\text{NH}_4)_2\text{S}_2\text{O}_8$, was added into the mixture dropwise and the reaction was allowed to continue for 5 h at room temperature. Resulting PANi/SD was filtered, washed with distilled water, and dried in an oven at 60°C. In order to increase the reproducibility of the results, PANi/SD was sieved before use. Particles of 0.355mm size were selected for adsorption experiments. Batch mode studies were conducted with fixed amounts (0.1 g to 1.0 g) of adsorbents which were shaken separately in an aqueous solution of the dye (40 mL) of varying concentration (5–100 ppm) at room temperature for definite time periods. At the end of the pre-determined time intervals, the adsorbent was removed by simple filtration.

2.3. Determination of pH point of zero charge

Point of zero charge is of fundamental importance in environmental science. It determines how easily a substrate is able to adsorb potentially harmful ions. The pH point of zero charge (pH_{pzc}) was carried out by taking 50 mL of 0.01 M NaCl solution in different closed Erlenmeyer flasks. The pH of the solution (pH_0) in each flask was adjusted to values of 2, 4, 6, 8 and 10 by adding 0.1 M HCl or 0.1 M NaOH solutions. Then 0.5 g of the adsorbent was added and agitated in a shaker for 1 h and allowed to stay for 48 h to reach equilibrium with intermittent manual shaking. Then the final pH value (pH_f) of the supernatant liquid was noted. The difference between the initial and final pH values ($\Delta\text{pH} = \text{pH}_0 - \text{pH}_f$) was plotted against the pH_0 . The point of intersection of the resulting curve at which $\Delta\text{pH} = 0$ gave the pH_{pzc} (M.S. Onyango *et al.*, 2004; V.C. Srivastava *et al.*, 2008)

2.4. Adsorbate

The dyes used were Reactive Red 43 (RR43) and Direct Orange 85 (DO85) which are anionic in nature. The stock solution was prepared by dissolving 1 g of dye in water and up to 1000 mL using double distilled water. The concentration of the dye solution was determined by using UV-Spectrophotometer (Elico make BL198) at its wavelength (503 nm for Reactive red 43 and 483 nm for Direct Orange 85).



Reactive red 43 Direct Orange 85

Dyes concentrations in the filtrate solutions were estimated by measuring the absorbance at maximum wavelength of the dye and computed from the calibration curves. The following equations were used to calculate the percentage of adsorption and the amount of adsorbed (RR43, DO85) respectively:

$$Adsorption = \frac{(C_0 - C_e)}{C_0} \times 100 \quad (1)$$

$$\frac{X}{m} = \frac{(C_0 - C_e)V}{m} \text{ Or } \frac{X}{m} = \frac{R \times C_0 \times V}{100 m} \quad (2)$$

where C_0 and C_e are the initial and equilibrium concentrations (mg L^{-1}) of (DO85, RR43), respectively, X/m is the amount of dye adsorbed onto a unit amount of the adsorbent (mg g^{-1}) at equilibrium, V is the volume (L) of the solution used in the adsorption experiment, and R is the percentage of dye removal.

3. Results and discussion

3.1. Characterization of the adsorbent

FT-IR spectrum of the **sawdust (SD)** (Figure 1) showed the most prominent peaks in the spectrum originate from hydroxyl group, which was probably attributed to adsorbed water (3854 cm^{-1}) and CH_2 and CH_3 asymmetric and symmetric stretching vibrations (2871 cm^{-1}). The spectrum of the **MWSD** also displayed number of peaks corresponding to the presence of many functional groups: NH stretch (3300 cm^{-1}), C=O stretching (1733 cm^{-1}), CO chelate stretching (1653 cm^{-1}), secondary amine (1507 cm^{-1}), symmetric bending of CH_3 (1457 cm^{-1}), CH_2 bending (1428 cm^{-1}), C-N vibration in primary amide (1368 cm^{-1}), C-O stretching (1272 cm^{-1}), O-H bending (1245 cm^{-1}), C-O antisymmetric stretching (1162 cm^{-1}), stretching of the many C-OH and C-O-C bonds (1054 cm^{-1}) [Stuart], C-H (835 and 897 cm^{-1}), Al-OH deformation (787 cm^{-1}), Al-O deformation (671 cm^{-1}) and SiO (541 cm^{-1}). On comparing spectrum of **MWSD** with modified **MWSD**, it could be seen that there were strong characteristic stretching vibration absorption band of carboxyl group (1732 cm^{-1}) and C-N vibration of primary amide (1384 cm^{-1}). It reflected the result of modified **sawdust** (Figure 1). The spectrum of reactive red 43 (RR 43), direct orange 85 (DO85) loaded **MWSD** and treated **MWSD** also exhibited small shift in some bands and some bands were disappeared. The intensity of the peaks were either minimized or shifted slightly as shown in Figure (1). These changes observed in the spectrum indicated the possible involvement of these functional groups on the surface of the **MWSD** and treated **MWSD** in adsorption process.

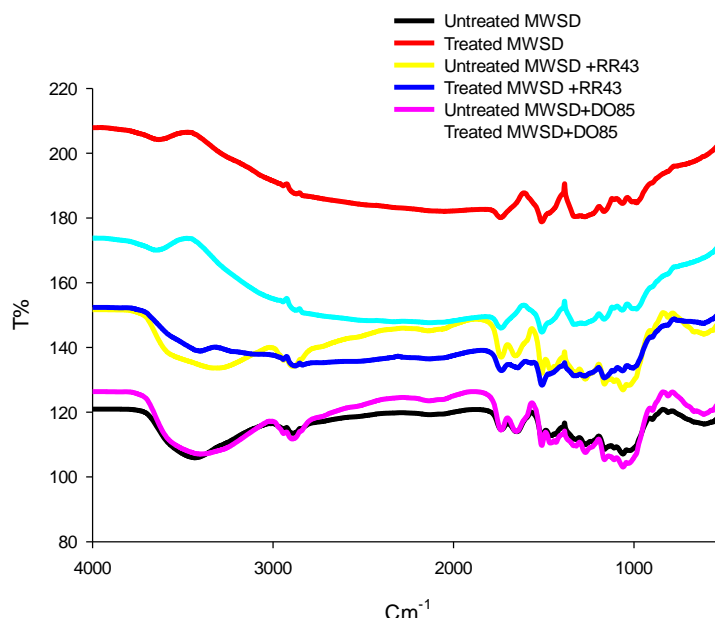


Fig. (1): FT-IR spectrum of both (MWSD) and (TMWSD), (MWSD adsorption by RR43 and DO85) and (TMWSD adsorption by RR43 and DO85 system).

Scanning electron microscopy (SEM) is known as an efficient technique for investigation and evaluation of the surface morphology of adsorbed. SEM of both untreated (MWSD) and treated

MWSD are shown in Fig. (2,3). Scanning electron microscope was used to investigate the surface morphology of MWSD and TMWSD as shown in Figure (2). The SEM image before dye adsorption revealed the rough surface of MWSD and TMWSD. The rough surface micrograph shows ridge like structure within which the presence of the macro pores were clearly noticeable. These rough surfaces and the macro pores were responsible for the high surface area, making MWSD and TMWSD a good adsorbent. The SEM image of TMWSD after adsorption RR 43 or DO85 showed smooth surface because the dye molecules were trapped and adsorbed on its surface Fig.(3,4).

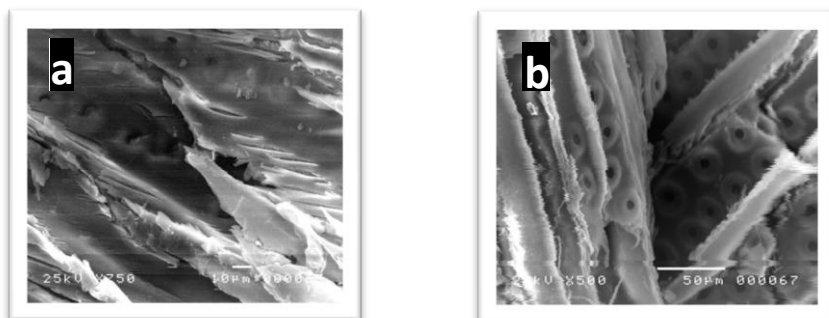


Fig.(2). SEM of both a-untreated (MWSD) and b- treated maple wood sawdust (TMWSD) .

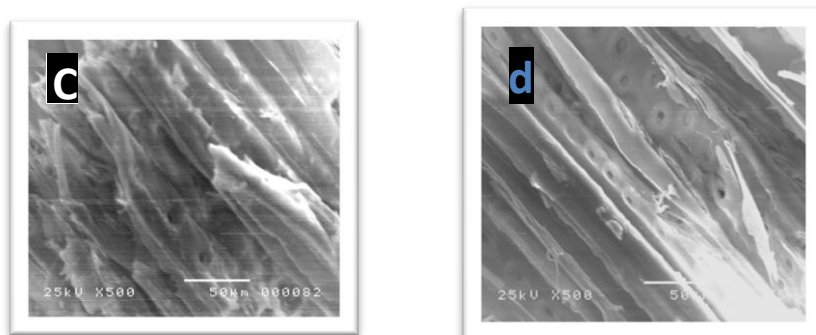


Fig.(3). SEM of untreated maple wood sawdust (MWSD) adsorption by c- DO85 and d-RR43 system.

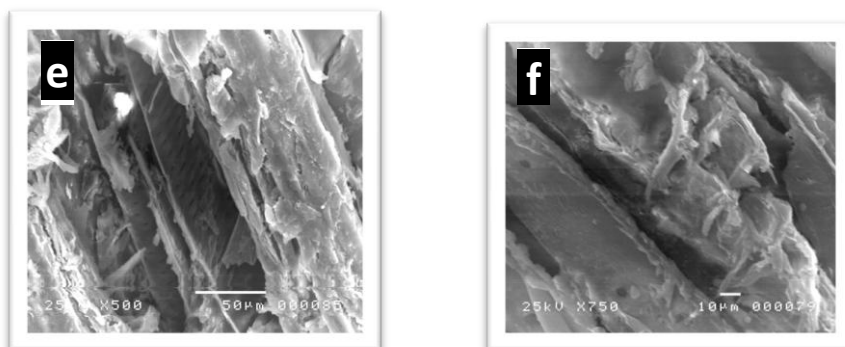


Fig.(4). SEM of treated maple wood sawdust (MWSD) adsorption by e- DO85 and f-RR43 system.

3.2. The effect of pH on the adsorption process

Fig. (5a) shows the plot of point of zero charge (pH_{pzc}) for the tow adsorbents (MWSD and TMWSD). The pH_{pzc} is a point at which the surface acidic (or basic) functional groups no longer contribute to the pH value of the solution. The pH_{pzc} of MWSD and TMWSD were found to be 6.32 and 4.32 respectively. It can be concluded that saw dust modified with polyaniline acidic surface since pH value of point of zero charge for TMWSD is at a lower pH compared to the value reported for MWSD. The surface acidity was due to the introduction of several oxygen-containing functional groups (P.C.C. Faria *et al.*, 2004).

To investigate the effect of pH on the RR43 and DO85 adsorption, RR43 and DO85 solution (40 mL, $c = 15\text{ppm}$) was treated with 0.7gm portions of dried sorbent (MWSD, PAni/MWSD) at various pH (1–10)(Fig.5b) As can be seen, the highest sorption percentage of RR43 and DO85 was observed for PAni/MWSD at pH values from 4 to 8. It is interesting to note that removal efficiency of MWSD is a popular and well established adsorbent in dye removal. However, its application in textile waste water treatment has been limited due to its high cost and poor regenerate ability. Removal of RR43 and DO85 using the introduced adsorbent is also higher compared to both MWSD at pH values from 4–8. Removal of dyes by PAni/MWSD might be mostly due to the strong intermolecular interactions (e.g. H-bonding) of RR43 and DO85 with the polymer. The same reason can be proposed for RR43 and DO85 removal by MWSD which has different functional polar groups in its constituent (e.g. lignin, cellulose, hemicellulose) (Lebo *et al*, 2001). Adsorption ability of MWSD is mainly due to its porosity and great surface area which helps to entrap adsorbates such as dye molecules.

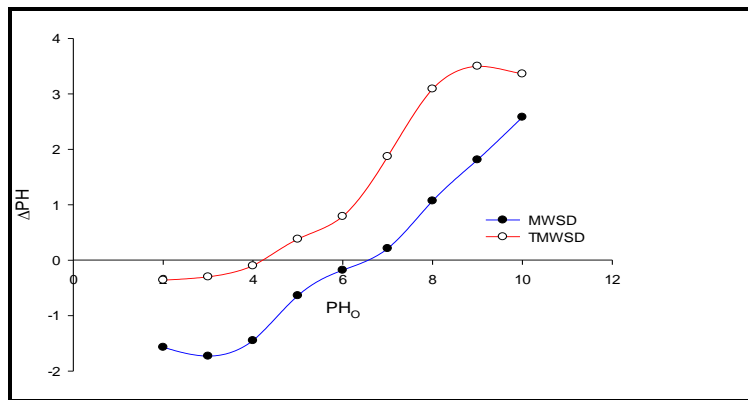


Fig. (5a)The zero point charge of MWSD and TMWSD.

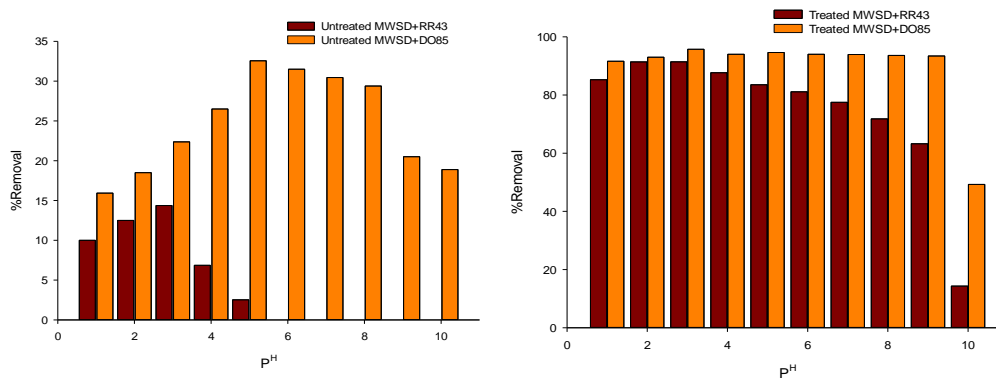
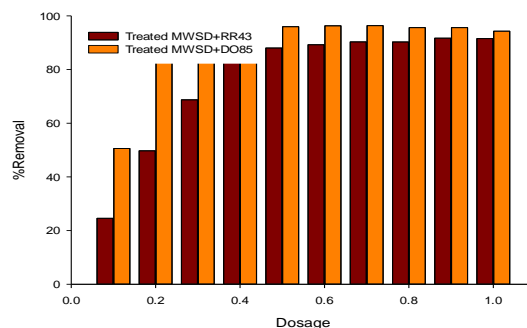


Fig.(5b)Effect of pH on the removal of RR43 and DO85: MWSD, PAni/MWSD.

3.3Effect of adsorbent dosage

In these experiments, RR43 and DO85 solution (40 mL, $c = 15\text{ppm}$) was treated with

5



different amounts of the selected adsorbent (MWSD, PANi/MWSD) (0.1–1.0 g). As seen from the results depicted in Fig. 6, higher sorption percentage of RR43 and DO85 was observed for PANi/MWSD for all examined sorbent dosages. Increase of removal percentage with the increasing adsorbent dose can be due to the higher adsorption sites available for interaction with the RR43 and DO85 molecules. It is evident that RR43 and DO85 removal percentage observed for PANi/MWSD is even higher than for MWSD which is a well established and commonly used adsorbent for decolorization. However, its high cost has limited its use considerably.

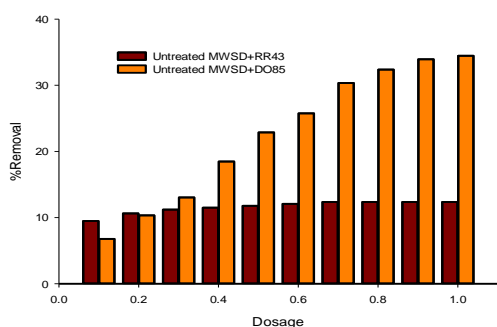


Fig. 6. Effect of adsorbent dosage on the removal of RR43 and DO85: MWSD, PANi/MWSD.

3.4. Effect of initial concentration

As our results show, at any C_0 of DO85 and RR43, higher sorption percentage was observed for PANi/MWSD compared to uncoated MWSD and a comparable or higher value of DO85 than that for RR43. High removal percentage of DO85 and RR43 using polyaniline might be due to high affinity and strong intermolecular interactions between (RR43, DO85) diazo groups ($-N=N-$), and polyaniline polymers which contain alternative imine and amino groups in their structures (Figs. 7). (Reza Ansari* and Zahra Mosayebzadeh, 2011).

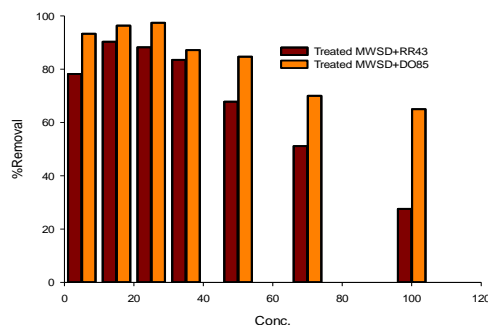
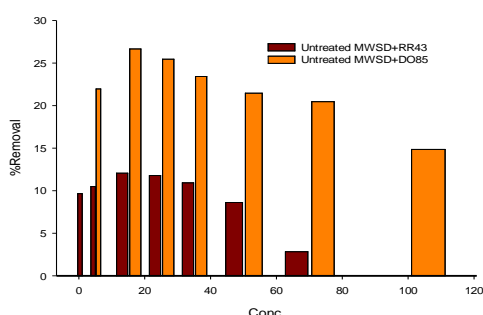


Fig.7. Effect of initial concentration of RR43 and DO85 (ppm) on the adsorption by MWSD, PANi/MWSD.).

3.5. Effect of contact time

DO85 and RR43 solution (40 mL, $C = 15$ ppm) was treated with 0.7 g of selected adsorbent (MWSD, PANi/MWSD) for different periods of time (5–120 min) with stirring at room temperature. Results of the adsorption obtained from the analysis of unabsorbed RR43 and DO85 solution are shown in Fig. 8. The results indicate higher removal efficiency observed for PANi/MWSD at all exposure times compared to SD adsorbents. Removal of RR43 and DO85 using PANi/MWSD is also very favorable from the kinetic point of view. Removal of RR43 and DO85 higher than 90 % occurred at the initial stage of exposure.

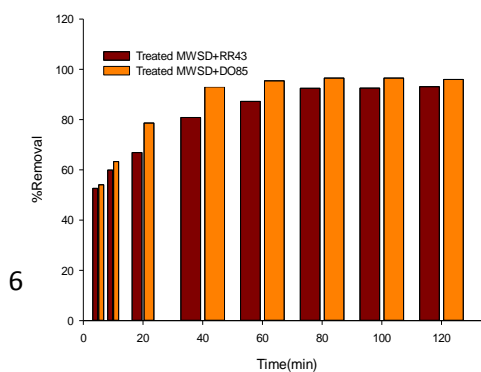
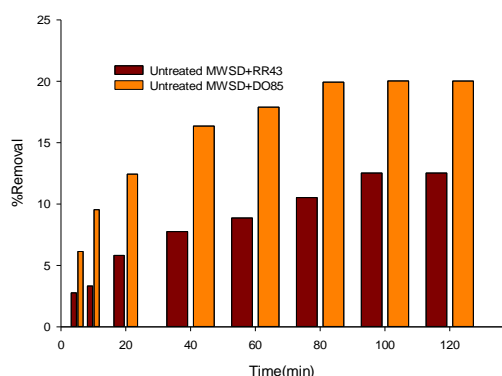


Fig. 8. Effect of contact time on the removal percentage of RR43 and DO85 (ppm) on the adsorption by MWSD, PA尼/MWSD.)

3.6. Kinetics modeling

Study of removal kinetics is important to evaluate adsorption dynamics. In order to determine the mechanism of adsorption processes such as chemical reactions and removal, the pseudo-first-order adsorption and the pseudo-second-order were used to examine the experimental data (Ho, 2004; Ho & Chiang, 2001; Ho & McKay, 2004). Adsorption of RR43 and DO85 on MWSD and PA尼/MWSD at different conditions was employed in the pseudo-first-order and pseudo-second-order models, and the rate constants of the first-order adsorption (k_1) and the rate constants of the second-order adsorption (k_2) were estimated, respectively.

3.6.1. Pseudo first order model

Lagergren kinetic equation describes the adsorption of liquid–solid systems based on solid capacity. In order to distinguish kinetic equations based on concentration of the solution and adsorption capacity of the solid, Lagergren first-order rate equation is termed as a pseudo-first-order reaction. The pseudo-first-order rate equation of Lagergren can be written as follows:

$$\log\left(\frac{q_e}{q_e - q_t}\right) = \log q_e - \frac{k_1}{2.303} \times t \quad (3)$$

Where q_e and q_t are the amounts (mg/g) of dye adsorbed at equilibrium and at time (t) respectively.

3.6.2. Pseudo second order model

The pseudo-second-order rate expression is based on the sorption capacity of solids but contrary to the previous model it describes chemisorption's over the whole adsorption time. The pseudo-second-order rate equation of McKay can be given in the following form:

$$\frac{t}{q_t} = \frac{1}{k_2 q_e^2} + \frac{1}{q_e} \quad (4)$$

where k_2 is the equilibrium rate constant of the pseudo-second order ($\text{g mg}^{-1} \text{min}^{-1}$). Plots of t/q_t versus t should give straight lines where slopes and intercepts are $1/q_e$ and $1/k_2 q_e^2$, respectively. Values of the rate constant k_2 and sorption capacity q_e can be calculated from these parameters. The resulting data summarized in Table 1 show that using the pseudo-second order kinetic model, the experimental sorption capacity q_e (exp) values are very close to the calculated sorption capacity q_e (calc). Kinetic data and correlation coefficients (R^2) confirm that sorption of RR43 and DO85 on MWSD and PA尼/MWSD follow the pseudo-second order kinetics model. The pseudo second order model is based on the assumption that the rate-limiting step is a chemical sorption between the adsorbate and adsorbent. This provides the best correlation of the data for all the three adsorbents.

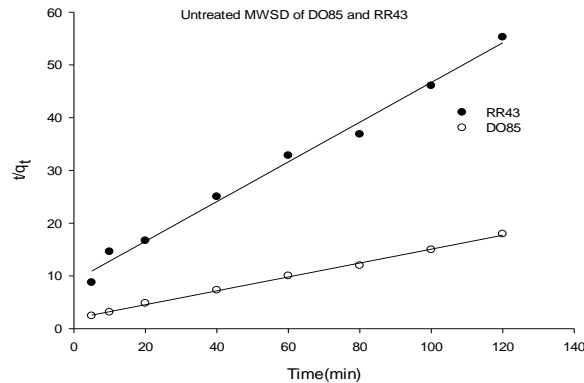


Fig.9.Pseudo second order plot for the adsorption of DO85 and RR43 onto MWSD.

Table 1.Adsorption kinetic parameters of RR43 and DO85 onto MWSD and PAni/MWSD

Dyes	Calculation						Experim ental
	The pseudo-first-order			The pseudo-second order			
	k_1 (min ⁻¹)	$q_{e,cal}$ (mg/g)	R ²	$K_2 \times 10^{-4}$ (g/mg min)	$q_{e,cal}$ (mg/g)	R ²	
DO85+MWSD	0.0149	1.413	0.9968	0.00912	7.593	0.9990	6.6857
DO85+TMWSD	0.0375	0.692	0.9864	0.00643	31.153	0.9997	29.611
RR43+ MWSD	0.0124	3.75	0.9966	0.0157	2.656	0.9954	2.1714
RR43+TMWSD	0.0174	0.888	0.9566	0.00251	13.755	0.9977	11.028

3.6.3. Elovich model

One of the most useful models for the studies of activated chemisorption is the Elovich equation. It is generally expressed as (Chien and Clayton,1980)

$$dq_t/dt = a_{exp} (-\beta q_t) \quad (5)$$

where q_t is the amount of solute adsorbed at time t , a is the initial adsorption rate (mg g⁻¹ min⁻¹) and β is the desorption constant (g mg⁻¹) during any one experiment. The Elovich equation can be simplified by assuming a $\beta t \gg 1$ and applying the boundary conditions $q_t=0$ at $t=0$ and $q_t=q_t$ at $t=t$. Eq. (5) becomes:

$$q_t = 1/\beta \ln(a\beta) + 1/\beta \ln(t) \quad (6)$$

The Elovich constants a and β can be obtained from the plot of q_t vs. $\ln(t)$.

3.6.4. The intraparticle diffusion model

The intraparticle diffusion model (Weber *et al.*,1963) is characterized by a linear relationship between the amounts adsorbed (q_t) and the square root of the time and is expressed as

$$q_t = (K_{id})t^{0.5} \quad (7)$$

where q_t (mg/g) is the amount of metal ions adsorbed at time t (min) and K_{id} is the initial rate of the intraparticle diffusion (mg (g min^{0.5})⁻¹). The rate constant of intraparticle diffusion K_{id} was determined by plotting q_t as a function of the square root of the time.

The pseudo first order model and Elovich model did not apply throughout all the contact times for all the two adsorbents. The calculated q_e values are lower than the experimental value.

The graph of q_t vs. $t^{0.5}$ shows a non-linear distribution of points, with two distinct portions (Figure not shown). The first, sharp portion is the external surface adsorption or instantaneous adsorption stage. The second linear portion indicates the existence of intraparticle diffusion in the process. Since the first portion is completed within 10 min, it can be neglected and then the stage of intraparticle diffusion control is attained and continues from 10 min to 1 h. The anionic dyes are slowly transported through the pores of the particle and is finally retained in the micropores. In general, the slope of the line in 2 portions is called as intraparticle diffusion rate constant. The rate constants of intraparticle diffusion (K_{id}) along with their regression coefficient are shown in Table 2. The K_{id} values led to the conclusion that intraparticle diffusion is the rate determining step in the adsorption of RR43 and DO85 on MWSD and PAni/MWSD. (Helen and Lima Rose, 2010).

Table (2) Estimated Elovich model and Intraparticle diffusion model kinetic parameters for DO85, RR43 dye adsorption by (MWSD) and (PAni/MWSD).

Dyes	Elovich model			Intraparticle diffusion model	
	β (g mg ⁻¹)	α (mg g ⁻¹ min ⁻¹)	R ²	K_{id} (mg g ⁻¹ min ^{-0.5})	R ²
DO85+MWSD	0.5259	0.6239	0.9989	0.5327	0.9630
DO85+TMWSD	6.8106	0.1772	0.9929	1.5248	0.9101
RR43+ MWSD	0.4020	1.8604	0.9852	0.2005	0.9760
RR43+ TMWSD	2.5340	0.3612	0.9889	1.0422	0.9876

3.7. Adsorption isotherms

The isotherm experiments were carried out for known concentration at pH value 6.0 for a concentration range of 5-100ppm. All solutions have a fixed specific mass of MWSD (0.7gm). The experimental data were fitted to various models such as Langmuir, Freundlich and Temkin.

3.7.1. Langmuir isotherm model

$$\frac{1}{X} = \frac{1}{X_m} + \frac{1}{bX_m C_e} \quad (8)$$

where, C_e is the equilibrium concentration of the dye solution (mg L^{-1}), X is the amount of dye sorbed by the adsorbent (mg g^{-1}), X_m is the maximum amount of dye sorbed, $b/(\text{L mg}^{-1})$ is a Langmuir constant for the energy of sorption. Values of b and X_m were calculated from the slope and intercept of the linear plot. The Langmuir model deals with monolayer adsorption and constant adsorption energy.

From Table (3) the sorption capacity, X_m , which is a measure of the maximum sorption capacity corresponding to complete monolayer coverage, showed that the adsorbent had a mass capacity and the adsorption coefficient, b Langmuir constant for the energy of sorption for DO85 greater than RR43. This observation was probably due to its having more active sites.

Furthermore, the essential characteristics of a Langmuir isotherm can be expressed in terms of a dimensionless separation parameter, the type of isotherm and is defined by the following equation:

$$R_L = \frac{1}{1 + bC_0} \quad (9)$$

Where b Langmuir isotherm constant; C_0 initial dye concentration. The value of R_L indicates the shape of the isotherms to be either unfavorable ($R_L > 1$), linear ($R_L = 1$), favorable ($0 < R_L < 1$) or irreversible ($R_L = 0$). The separation parameters for the two dyes are less than unity indicating that MWSD adsorbent is an excellent adsorbent for the two dyes.

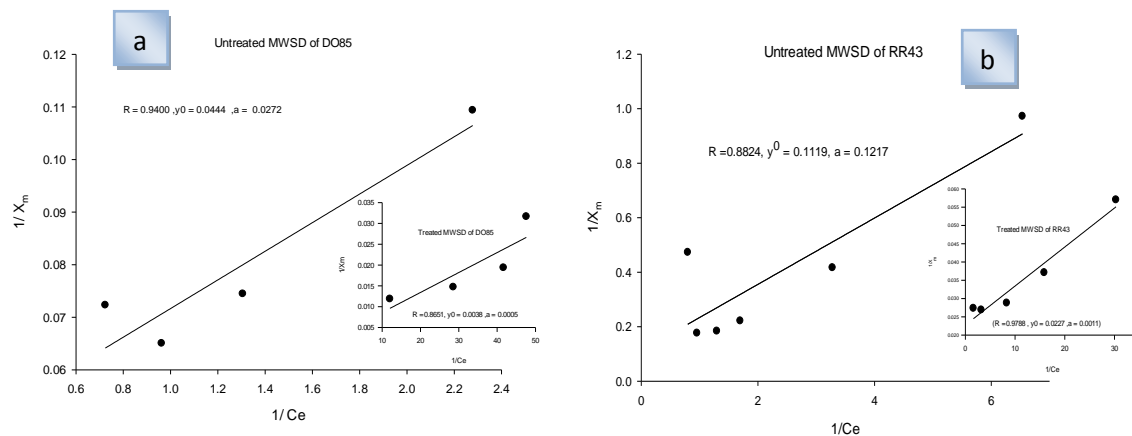


Fig. 10. Langmuir isotherm obtained for sorption of DO85 (a) and RR43 (b) by MWSD and treated MWSD

Table 3. Isotherm constants for the adsorption of RR43 and DO85 onto MWSD and PANi/MWSD.

Dyes	Langmuir				R^2	Freundlich			Temkin		
	b	$1/X_m$	X_m	R_L		n	K_f	R^2	b_T	K_T	R^2
DO85+ MWSD	0.0011	0.0444	22.52	0.7102	0.940	1.1495	0.9552	0.9268	0.0001	0.0014	0.8603
DO85+ TMWSD	0.1217	0.0038	263.16	0.9925	0.865	4.8616	0.0211	0.9593	0.0001	0.0144	0.9424
RR43+ MWSD	0.0005	0.1119	8.9366	0.3539	0.882	1.0117	0.9211	0.9823	0.0007	0.0018	0.9824
RR43+ TMWSD	0.0272	0.0227	44.053	0.9852	0.978	1.6723	0.2339	0.8660	0.0009	0.0106	0.9128

3.7.2. Freundlich isotherm

The Freundlich model was chosen to estimate the adsorption intensity of the sorbate on the sorbent surface. The Freundlich model is represented in equation

$$\log \frac{X}{m} = \log K_f + \frac{1}{n} \log C_e \quad (10)$$

where X/m is the equilibrium adsorption capacity (mg g^{-1}), C_e is the equilibrium or residual concentration (mg L^{-1}) of dye in the solution, and K and $1/n$ are empirical Freundlich constants indicating sorption capacity of the adsorbent and intensity of the adsorption (mg g^{-1}), respectively. In the Freundlich adsorption system, values of n and K were calculated from the slope and intercept of the linear plot of $\log X/m$ against $\log C_e$.

The experimental data from the batch sorption study of the anionic dyes such as RR43 and DO85 by MWSD were illustrated in Table (3) and plotted logarithmically using the linear Freundlich isotherm equation. The linear Freundlich isotherm constants for RR43 and DO85 are presented in table (3). The ultimate adsorption capacity K_f , of the adsorbent was calculated from the isothermal linear regression equation. The increase of negative charge due to the presence of $-\text{COOH}$, $-\text{SO}_3\text{H}$, and $-\text{OH}$ groups on the surface of the adsorbent that enhances the electrostatic force like vanderwaal's between the adsorbent surface and dye ion, which increases the adsorption of DO85. The K_f value of DO85 is greater than that of RR43, suggesting and confirming that DO85 has greater adsorption tendency towards the maple wood sawdust than the other dye. The values of n were found to be greater than 1 which may be attributed to the distribution of surface sites or any factor responsible for a decrease in dye maple woodsawdust interaction with increasing surface density.

3.7.3. Temkin isotherm model

The Temkin adsorption isotherm model was chosen to evaluate the adsorption potentials of the adsorbent for adsorbates. The linear form of the Temkin isotherm model as shown in equation 11 was plotted as q_e against $\ln C_e$.

$$q_e = \frac{RT}{b_T} \ln K_t + \frac{RT}{b_T} \ln C_e \quad (11)$$

where the $1/b_T$ indicates the adsorption potential of the adsorbent and K_t is the Temkin isotherm constant ($\text{dm}^3 \text{g}^{-1}$). The experimental data from the batch sorption study of the three dyes by maple woodsawdust are illustrated in Table (3). A plot of q_e versus $\ln C_e$ yielded linear lines which enable the determination of the isotherm constants K_t and b_T from intercepts and slopes respectively.

4. Conclusion

In this study we investigated The removal of two anionic dyes DO85 and RR43 using MWSD and PAni/MWSD. The results showed that the adsorption capacity at equilibrium of both dyes was favorable at neutral pH. The adsorption data fitted well the Langmuir isotherm, with a maximum monolayer adsorption capacity 63.16 mg g^{-1} and 44.053 mg g^{-1} for the DO85 and RR43, respectively. The adsorption kinetics was best described by the pseudo-second-order kinetic model. In addition, the kinetic data of the adsorption process had a good agreement with the pseudo-second order model. From the results of the

present study, it is concluded that PAni/MWSD was found to be suitable adsorbent for the removal of both (DO85) and reactive (RR43) dyes (anionic dyes).

Reference

- Chen, D., Lei, S., Chen, Y., 2011a. A single polyaniline nanofiber field effect transistor and its gas sensing mechanisms. *Sensors* 11, 6509-6516.
- Chien, S.H. Clayton, W.R. (1980) *Soil Sci. Soc. Am. J.* 44 265–268.
- Crini, G., 2006. Non-conventional low-cost adsorbents for dye removal: a review. *Bioresour. Technol.* 97, 1061-1085.
- Goes, M.M., Keller, M., Oliveira, V.M., Villalobos, L.D.G., Moraes, J.C.G., Carvalho, G.M., 2016. Polyurethane foams synthesized from cellulose-based wastes: kinetics studies of dye adsorption. *Ind. Crops Prod.* 85, 149-158.
- Garg VK, Gupta R, Kumar R, Gupta RK., 2004. Adsorption of chromium from aqueous solution on treated sawdust. *Bioresour Technol.* 92:79.
- Ho, Y. S., & Chiang, C. C. (2001). Sorption studies of acid dye by mixed sorbents. *Adsorption*, 7, 139–147. DOI:10.1023/A:1011652224816.

- Ho, Y.-S. (2004). Citation review of Lagergren kinetic rate equation on adsorption reactions. *Scientometrics*, 59, 171–177.
- Jaymand, M., 2013. Recent progress in chemical modification of polyaniline. *Prog. Polym. Sci.* 38, 1287e1306.
- Kalavathy, M. H. Lima Rose Miranda (2010). Comparison of copper adsorption from aqueous solution using modified and unmodified Heveabrsiliensis saw dust. *Desalination* 255 165–174
- Kamran Zarrini, Abd Allah Rahimi, Farzaneh Alihosseini*, Hossein Fashandi., 2017. Highly efficient dye adsorbent based on polyaniline-coated nylon-6 Nanofibers.
- Lebo, S. E., Jr., Gargulak, J. D., & McNally, T. J. (2001) Lignin. In J. I. Kroschwitz, & M. Howe-Grant (Eds.), *Kirk–Othmer encyclopedia of chemical technology* (5th ed. Vol. 15, pp. 1–24). New York, NY, USA: Wiley. DOI:10.1002/0471238961.1209071412, 0914.a01.pub2.
- Lee, L.Y., Gan, S., Yin Tan, M.S., Lim, S.S., Lee, X.J., Lam, Y.F., 2016. Effective removal of Acid Blue 113 dye using overripe Cucumissativus peel as an eco-friendly biosorbent from agricultural residue. *J. Clean. Prod.* 113, 194e203.
- Maas, R., Chaudhari, S., 2005. Adsorption and biological decolorization of azo dye Reactive Red 2 in semicontinuous anaerobic reactors. *Process Biochem.* 40, 699e705.
- Onyango, M.S. Y. Kojima, O. Aoyi, E.C. Bernardo, H. Matsuda, J. *Colloid Interface Sci.* 279, (2004) 341–350.
- P.C.C. Faria, J.J.M. Orfao, M.F.R. Pereira, *Water Res.* 38 (2004) 2043–2052.
- Rafatullah, M., Sulaiman, O., Hashim, R., Ahmad, A., 2010. Adsorption of methylene blue on low-cost adsorbents: a review. *J. Hazard. Mater.* 177, 70e80.
- Reza Ansari, Zahra Mosayebzadeh. 2011. Application of polyaniline as an efficient and novel adsorbent for azo dyes removal from textile wastewaters *Chemical Papers* 65 (1) 1–8 (11) DOI: 10.2478/s11696-010-0083-x
- Robinson, T., McMullan, G., Marchant, R., Nigam, P., 2001. Remediation of dyes in textile effluent: a critical review on current treatment technologies with a proposed alternative. *Bioresour. Technol.* 77, 247e255.
- Shukla A, Zhang YH, Dubey P, Margrave JL, Shukla SS., 2002. The role of sawdust in the removal of unwanted materials from water. *J Hazard Mater*;95:137.
- Srivastava, V.C. I.D. Mall, I.M. Mishra, 2008. *Chem. Eng. Process.* 47 1269–1280.
- Syed, A.A., Dinesan, M.K., 1991. Review: polyaniline a novel polymeric material. *Talanta* 38, 815e837.
- Venkat S. Mane, P.V. Vijay Babu., 2013. Kinetic and equilibrium studies on the removal of Congo red from aqueous solution using Eucalyptus wood (*Eucalyptus globulus*) saw dust *Journal of the Taiwan Institute of Chemical Engineers* 44 81–88.
- Weber, W.J., Morris, J.C. *Sanit. J. Eng. Div. (1963) Am. Soc. Civ. Eng.* 89 31–60.

الملخص العربي

للبحث العلمي بعنوان

Application of modified Maple Wood Saw Dust with polyaniline for the removal of Anionic Dyes From waste water : Kinetics and Isotherm Studies

(في هذا العمل، يتم تطبيق تغطية البولي انيلين على نشارة الخشب وذلك لإزالة الأصباغ الأيونية وهي عباره عن صبغة الأحمر المنشط 43 (صبغة 43) و البرتقالي المباشر 85 (صبغة 85) من المحاليل المائية. وقد تمت دراسة ذلك من خلال التحليل الطيفي للأشعة تحت الحمراء (FTIR)، المساح الضوئي المجهرى الإلكتروني (SEM). كما تم دراسة آثار بعض النظريات الهامة مثل الرقم الهيدروجيني، والتركيز الابتدائي، والجرعات الماصة، ووقت الاتصال على امتصاص محلول الأصباغ الأيونية. ومن أجل الحصول على مقارنة أفضل، أجريت تجارب الامتصاص أيضا باستخدام نشارة الخشب المغطاه بالبولي انيلين (PANi/MWSD) وبدون تغطيه (MWSD). وقد وجد أن نشارة الخشب المغطاه بالبولي انيلين يمكن استخدامها لإزالة الأصباغ الأيونية مثل صبغة الحمراء النشطة 85 و البرتقالي المباشر 43 الأصباغ من المحاليل المائية بكفاءة عالية. تم تحليل البيانات التجريبية من قبل نماذج لانجمير، فريندليش و تمكين للامتزاز. كما أثبت من النظريات الحركية لامتزاز الأصباغ الأيونية للممتازات المختارة. تطبيق نشارة الخشب المعدلة مع بوليانيلين لإزالة الأصباغ الأيونية والهامة جدا لمعالجة مياه الصرف الصحي.)

أسماء المؤلفين:

- 1- أ.م.د/عبير أحمد إمام استاذ مساعد الكيمياء الفيزيائية –جامعة الأزهر
- 2- أ.م.د/نورا هلال استاذ مساعد الكيمياء الفيزيائية –جامعة الأزهر
- 3- أ.د/أمينة حمادة استاذ الكيمياء الفيزيائية –جامعة الأزهر
- 4- أ.د/نجوي بدوي استاذ الكيمياء الفيزيائية –جامعة الأزهر
- 5- الطالبه /يمني عبد المنعم محمد –جامعة الأزهر